Emittance Effects on Gain in *W*-Band TWTs

Bruce E. Carlsten, *Fellow, IEEE*, Kimberley E. Nichols,
Dmitry Yu. Shchegolkov, and Evgenya I. Simakov

***Abstract*— We consider the main effects of beam emittance on W-band traveling-wave tube (TWT) performance and gain. Specifically, we consider a representative dielectric TWT structure with ∼5 dB/cm of gain driven by a 5-A, 20-keV, sheet electron beam that is focused by a wiggler magnetic field. The normalized beam transverse emittance must be about 1 μm or lower to ensure that both the transport is stable and the gain is not degraded by the effective energy spread arising from the emittance. This emittance limit scales roughly inversely with frequency.**

***Index Terms*— Electron beams, millimeter-wave amplifiers, traveling-wave tubes (TWTs).**

I. Introduction

NOVEL *W*-band, and higher frequency, traveling-wave tubes (TWTs) are achieving new levels of power [1]–[6]. This power increase is enabled by an increase in beam current, which in turn leads to greater space-charge effects and increased beam transverse normalized rms emittance. A beam's emittance can be considered as a pressure that defocuses the beam, similar to space charge. Beam emittance can be caused by, for example, the transverse thermal spread of the electron emission at the cathode (see Fig. 1) or by the electron flow around a cathode shadow grid. The beam's evolution in the emittance-dominated regime is fundamentally different from that in the space-charge dominated regime and it can have a direct impact on a TWT's performance.

Emittance can affect beam interception during transport, as discussed in [7]–[9]. In addition, emittance can impact the stability of beam transport in periodic focusing structures and can degrade gain. Its effect on transport stability and gain, along with the intrinsic emittance growth in periodic focusing structures, are the focus of this paper. It is well known that emittance degrades the gain in free-electron lasers– due to the conservation of energy, a large emittance leads to an effective increased energy spread [10]. We will show that this same mechanism starts to become important for nominal *W*-band TWT parameters, and may be dominant for tubes with frequencies above *W*-band.

For this analysis, we consider the parameters associated with the photonic-bandgap (PBG) *W*-band TWT project at Los Alamos [11], [12]. The PBG slow-wave structure is shown in Fig. 2, where an elliptical electron beam with a high aspect ratio interacts with modes in a dielectric structure. The nominal beam parameters for this device are 5-A current, 20-keV energy, and 1-μm normalized rms emittance in the beam's narrow dimension. Periodic wiggler focusing is used to confine the beam within the narrow beam tunnel in the structure.

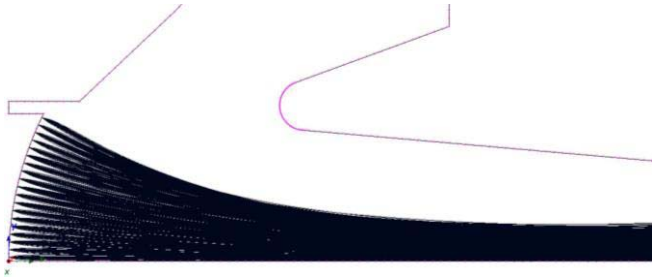

Fig. 1. Electron gun simulation showing the initial transverse beam velocity spread from the random thermal electronic motion at the cathode, leading to an initial beam emittance.

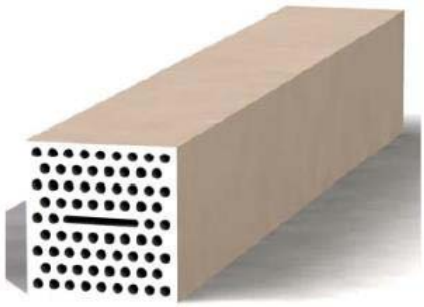

Fig. 2. Notional PBG slow wave structure. The white material is dielectric with dielectric constant of about 20. The dark areas are vacuum and are longitudinally uniform. A sheet electron beam is transported through the wide slot. The holes confine a TM_{11}-like mode over a wide bandwidth; other modes are not confined.

This paper is organized as follows. In Section II, we review relevant emittance concepts and provide background emittance definitions. In Section III, we estimate gain for an example dielectric PBG TWT based on simple arguments. In Section IV, we determine the maximum emittance that allows us to stably transport the beam through the beam tunnel. In Section V, we calculate how the gain is degraded by the beam emittance using a quasilinear gain analysis. and in Section VI, we calculate the possible emittance growth due to nonlinear effects in periodic focusing. Most novel *W*-band and higher frequency TWTs under investigation [1]–[6], [11], [12] are compact and at relatively low voltage ($\leq$20 keV), therefore, this analysis will be done nonrelativistically

Manuscript received July 22, 2016; revised September 16, 2016; accepted September 19, 2016. Date of current version October 20, 2016. This work was supported by the U.S. Department of Energy through the LANL/LDRD Program. The review of this paper was arranged by Editor L. Kumar.

The authors are with the Los Alamos National Laboratory, Los Alamos, NM 87545 USA (e-mail: bcarlsten@lanl.gov; knichols@lanl.gov; d_shcheg@lanl.gov; smirnova@lanl.gov).

Color versions of one or more of the figures in this paper are available online at http://ieeexplore.ieee.org.

Digital Object Identifier 10.1109/TED.2016.2612583

(except for the definitions in Section II). Extension to relativistic beam energies is straightforward.

II. Relevant Emittance Concepts

The emittance is defined in a transverse dimension (here for y) at a longitudinal position z along the TWT as

$$\varepsilon_{y,\text{norm}} = \gamma_b \beta_b \sqrt{\langle y^2 \rangle \langle y'^2 \rangle - \langle y y' \rangle^2} \tag{1}$$

where the brackets indicate ensemble averages, the primes refer to an axial derivative, and γ_b and β_b are the beam's relativistic mass factor and velocity normalized to the speed of light c, respectively. We are most interested in emittance effects for the case where the beam is focused with a periodic magnetic field; here, we assume single-plane wiggler focusing (known as natural focusing), where the focusing is in the y-direction across the wiggler's gap. The conclusions are the same with two-plane focusing and for periodic focusing relying on the axial magnetic field [i.e., periodic permanent magnet (PPM) focusing] [13].

Using $X^2 = \langle x^2 \rangle$ and $Y^2 = \langle y^2 \rangle$ for the rms beam sizes, the vertical envelope equation for an elliptical beam is [13]

$$Y'' = -Y \left(\frac{e}{cm\gamma_b \beta_b} \right)^2 B^2 + \frac{I/I_A}{\gamma_b^3 \beta_b^3} \frac{1}{X+Y} + \frac{\varepsilon_{y,\text{norm}}^2}{Y^3 \gamma_b^2 \beta_b^2} \tag{2}$$

where e and m are the electronic charge and mass, respectively, B is the rms focusing magnetic field, I is the beam current, and I_A is ~17 kA. Importantly, the emittance defocusing term in the envelope equation dominates when $\varepsilon_{y,\text{norm}}^2 > (I/I_A) Y^3 / \gamma_b \beta_b (X+Y)$, which is achieved for small enough beam sizes. For nominal beam parameters for W-band TWTs (5-A, 20-keV electron beams with transverse rms sizes of 0.1 mm × 1 mm), the emittance defocusing dominates if it is greater than 1 μm. Since thermionic electron guns with these parameters typically have emittances of 1 μm to a few micrometers, W-band TWTs are largely operating in the emittance-dominated regime.

The thermal energy of the emission from the cathode provides a lower limit on the beam's transverse rms emittance. The normalized thermal emittance is given by [14]

$$\varepsilon_{y,\text{therm}} = Y_{\text{cath}} \sqrt{\frac{kT}{mc^2}} \tag{3}$$

which, assuming a nominal temperature of 1200 K, leads to a lower emittance limit of about $\varepsilon_{y,\text{therm}} = 4.5 \times 10^{-4} Y_{\text{cath}}$. One way to keep the thermal emittance at or below the threshold of 1 μm is to have a moderately high emission current density, for instance, by using a long-life scandate cathode operating at 10 A/cm^2 [15]. A cathode edge radius of 4 mm ($Y_{\text{cath}} = 2$ mm) would then produce a 5 A electron beam with a thermal rms emittance of ~0.9 μm. Some moderate emittance growth is likely from the beam dynamics in the diode region, but that can be kept insignificant for low-perveance designs.

III. Nominal W-Band TWT Example

We can use a dielectric structure with a metallic boundary, see Fig. 3, as a representative example for the PBG slow-wave structure, where the metal boundary approximates the trapping

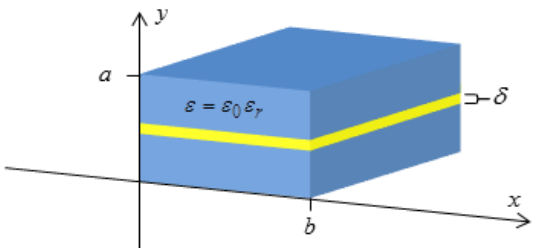

Fig. 3. Nominal PBG slow wave structure used in the analysis. Two blocks of dielectric with constant ε are separated by a vacuum gap δ shown in yellow. The external metallic boundary surrounding the structure is not shown.

effect of the PBG structure. (It is important to note that the height and width of the PBG structure will be larger than for a metal-clad dielectric structure.) We assume a 5-A, 20-keV beam that travels down a central beam tunnel with a gap of width δ. We can estimate the gain by treating the gap as a perturbation. The gain calculated in this way for this substitute structure compares reasonably well with the gain in our actual structures [12], numerically determined with CST Microwave Studio [16] (after some manipulation of the PBG geometry is made to keep the RF mode centered about the beam tunnel). This calculation has two purposes: 1) to identify the limit on the beam tunnel height (and thus the beam height itself), which is used for the stability analysis of the electron transport in Section IV and 2) to provide a characteristic gain formula to use in the analysis of emittance-based gain degradation in Section V.

We start by assuming that the electric fields for the TM_{11} mode in the dielectric are the same as if the tunnel is not present

$$\begin{aligned} E_z &= E_0 \sin\left(\frac{\pi x}{b}\right) \sin\left(\frac{\pi \hat{y}}{a-\delta}\right) e^{j(\omega t - \beta_1 z)} \\ E_x &= -\frac{j\beta\pi}{h^2 b} E_0 \cos\left(\frac{\pi x}{b}\right) \sin\left(\frac{\pi \hat{y}}{a-\delta}\right) e^{j(\omega t - \beta_1 z)} \\ E_y &= -\frac{j\beta\pi}{h^2 (a-\delta)} E_0 \sin\left(\frac{\pi x}{b}\right) \cos\left(\frac{\pi \hat{y}}{a-\delta}\right) e^{j(\omega t - \beta_1 z)} \end{aligned} \tag{4}$$

where the xy origin is at the lower left corner of the waveguide, $\hat{y} = y$ if $y \le (a-\delta)/2$ and $\hat{y} = y - \delta$ if $y \ge (a+\delta)/2$, and $h^2 = \beta_x^2 + \beta_y^2$, with $\beta_x = \pi/b$ and $\beta_y = \pi/(a-\delta)$. Note that $\beta_1 = (k_0^2 - \beta_x^2 - \beta_y^2)^{1/2}$ is the axial wavenumber of the cold dielectric waveguide mode without beam, where we define $k_0 = \omega(\varepsilon\mu_0)^{1/2}$. In addition, we will assume that the hot RF mode has an axial propagation constant $\beta = \beta_1 + \delta\beta$, where the complex value $\delta\beta$ is small compared with β_1 and its imaginary part is responsible for the structure's gain.

The structure's dielectric constant must be high to synchronize the beam velocity to the RF phase velocity. Next, we find that dielectric constant. Following that, finding the power flow, we calculate the coupling impedance and then the gain.

A. Dielectric Constant in the Representative PBG Structure

Assuming that the field is excluded from the beam tunnel, we find the dielectric constant from matching the mode's phase

velocity to the electron beam velocity

$$v_{\text{beam}} = v_{\text{phase}} = \frac{1}{\sqrt{\mu_0 \varepsilon}} \frac{1}{\sqrt{1 - f_c^2/f^2}} \tag{5}$$

where f is the mode's frequency and $\varepsilon = \varepsilon_0 \varepsilon_r$. The cutoff frequency is $f_c = (1/(2\sqrt{\mu_0 \varepsilon}))((1/(a-\delta))^2 + (1/b)^2)^{1/2}$ which gives us

$$\varepsilon_r = \frac{c^2}{v_{\text{beam}}^2} + c^2 \frac{\left(\frac{1}{a-\delta}\right)^2 + \left(\frac{1}{b}\right)^2}{4f^2}. \tag{6}$$

B. Coupling Impedance for the Dielectric Structure

The nonrelativistic Pierce parameter is $C^3 = ((I_{\text{beam}})/(4V_{\text{beam}}))K_{\text{int}}$, where the coupling impedance is $K_{\text{int}} = ((E_{\text{beam}}^2)/(2\beta_1^2 P_{\text{ave}}))$ [17], I_{beam} is the total current of the electron beam, and V_{beam} is the beam voltage. From the vacuum wave equation, the field at the center of the beam tunnel (and at the center of the electron beam) is related to the unperturbed structure mode field by

$$E_{\text{beam}} = E_z(x = b/2, y = a/2)\left[\cosh\left(\frac{\omega}{v_{\text{beam}}}\frac{\delta}{2}\right)\right]^{-1}. \tag{7}$$

The average power flow is

$$P_{\text{ave}} = \int_0^b \int_0^a \left(\frac{|E_x|^2 + |E_y|^2}{2\eta_{\text{TM}}}\right) dx \; dy \tag{8}$$

where the TM mode impedance is given by

$$\eta_{\text{TM}} = \sqrt{\frac{\mu_0}{\varepsilon}}\sqrt{1 - f_c^2/f^2}, \text{ or}$$

$$P_{\text{ave}} = E_0^2 \frac{\omega^2 \pi^2}{8\sqrt{\mu_0/\varepsilon}} \frac{\left(\frac{b}{a-\delta}\right) + \left(\frac{a-\delta}{b}\right)}{\left(\left(\frac{\pi}{a-\delta}\right)^2 + \left(\frac{\pi}{b}\right)^2\right)^2} \frac{\sqrt{\mu\varepsilon}}{v_{\text{beam}}}. \tag{9}$$

The coupling impedance is then

$$K_{\text{int}} = \frac{4\pi^2}{\varepsilon_r \varepsilon_0 \omega} \frac{1}{(\omega/v_{\text{beam}})^3} \frac{\frac{1}{(a-\delta)^2} + \frac{1}{b^2}}{(a-\delta)b} \times \left[\cosh\left(\frac{\omega}{v_{\text{beam}}}\frac{\delta}{2}\right)\right]^{-2}. \tag{10}$$

C. Gain in the Dielectric Structure

The gain in decibel is given by $G = A + BCN$ where A is the insertion loss (−9.54 dB) and N is the number of wavelength over a given distance [17]. Fig. 4 shows the gain at 95 GHz for different beam tunnel heights as a and b are changed, keeping the ratio $b/a = 5$ (with a 20-kV, 5-A beam) constant. Fig. 4 indicates that a maximum allowable dielectric height a is about 1.5 mm with a maximum tunnel height δ of about 0.5 mm to achieve ∼5 dB/cm. These rough estimates are in decent agreement with the detailed structure simulations [12]. For the analysis in the following, we note that $C = 0.009$ for a gain of 5 dB/m.

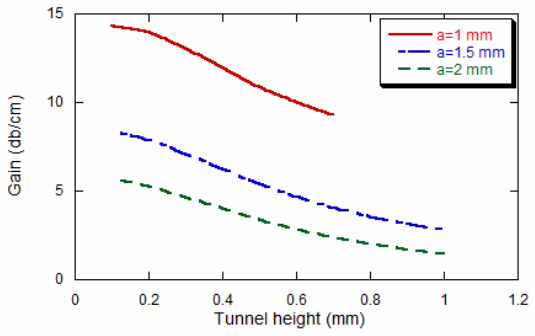

Fig. 4. Gain versus tunnel height δ for different dielectric heights a with the width fixed at five times the height. Although the approximations used are challenged for much of the red line and some of the blue line, these curves do indicate that a maximum tunnel height is about 0.5 mm and the maximum dielectric height is about 1.5 mm.

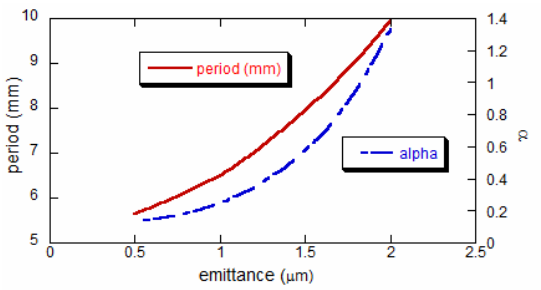

Fig. 5. Required wiggle period and resulting α stability parameter as a function of beam emittance, assuming a wiggler gap of 2.5 mm and an rms beam size of 0.075 mm × 0.5 mm.

IV. Emittance Impact to Stable Focusing

Beam emittance impacts the ability to stably focus the beam through such a narrow tunnel. Here, we assume that we are using a PPM focusing scheme, specifically a wiggler, instead of a solenoidal field, in order to eliminate the beam's edge curling due to the ExB drift [18]. The peak wiggle field for a permanent magnet wiggler with magnet block height $\lambda_w/2$, where λ_w is the wiggler magnet period, is closely approximated by

$$B_w = 1.723 B_r e^{-\pi g/\lambda_w} \tag{11}$$

where B_r is the remnant field (∼1.27 T for NdFeB and ∼0.9 for SmCo), and g is the gap between the magnet planes [19]. We can find the required magnetic field for balanced flow from the envelope equation (2) with $B_w = \sqrt{2}B$ (to have the same rms field strength). Assuming a minimum wiggler gap of 2.5 mm (to accommodate the entire height of the dielectric structure), we find the wiggle period λ_w from the equation above. The Mathieu stability requirement for wiggler focusing is [13]

$$\alpha = \left(\frac{\lambda_w^2}{8\pi^2 v_{\text{beam}}^2}\right)\left(\frac{e^2 B_w^2}{4m^2}\right) < 0.66. \tag{12}$$

The wiggle period and the stability parameter are shown as a function of beam emittance in Fig. 5, where the rms vertical beam size is about 15% of the tunnel height to minimize interception (a thorough study of interception in emittance-dominated transport can be found in [9]). For these conditions,

Fig. 5 indicates the emittance for low scalloping transport ($\alpha < 0.3$) must be <1.5 μm.

V. Gain Degradation Due to Emittance

Free-electron lasers operate in the emittance-dominated regime. It is well known that how beam emittance degrades their performance [10]—confining the beam increases the beam's transverse motion due to nonzero transverse emittance, which leads to an effective energy spread, which, in turn, degrades the beam-wave interaction. Similar degradation is possible in TWTs; in this section, we calculate the extent of this degradation.

Specifically, we derive an expression for the decrease in gain due to a beam's energy spread using a quasi-linear theory. This derivation largely follows Watkins original derivation [20] in order to find the modification to the usual TWT dispersion function, and then, we use a waterbag energy distribution (where the beam's energy distribution is uniform over some energy interval) to derive an expression for the gain as a function of rms energy spread. We assume that the gain only depends on rms quantities and not the exact beam distribution, which is a common and accurate assumption for accelerator and beam physics [21], [22].

We separate the distribution and density functions into dc and RF [with $\exp(j(\omega t - \beta z))$ dependence] components, $f_t(z, v, t) = f_{\rm dc}(v) + f_{\rm RF}(z, v, t)$ and $\rho_t(z, t) = \rho_0 + \rho_{\rm RF}(z, t)$, which are related by $\rho_{\rm RF}(z, t) = \int_{-\infty}^{\infty} f_{\rm RF}(z, v, t) dv$ and $\rho_0 = \int_{-\infty}^{\infty} f_{\rm dc}(v) dv$. As before, we assume that $\beta = \beta_1 + \delta\beta$ where $\delta\beta$ is very small and β_1 is the axial propagation constant of the cold RF mode. We also assume that the beam is synchronous, or $\beta_1 = \omega/v_{\rm beam}$. To simplify the derivation, we will additionally assume here that the electron beam fills the dielectric waveguide. The form of the degradation in gain for the case the beam is instead confined to a beam tunnel (as in Section III) is the same as will be found here, with the gain itself only differing by some geometrical factors close to unity.

We start with the linearized Vlasov equation

$$0 = \frac{\partial f_{\rm RF}}{\partial t} + v\frac{\partial f_{\rm RF}}{\partial z} - \frac{eE_z(z,t)}{m}\frac{\partial f_{\rm dc}}{\partial v} \tag{13}$$

where E_z is the axial electric RF field, to derive an electronic equation

$$j(\omega - \beta v) f_{\rm RF} = -\frac{eE_z(z,t)}{m}\frac{\partial f_{\rm dc}}{\partial v}. \tag{14}$$

The quasi-linear analysis is simple for a dielectric block. We use the driven wave equation for the vector potential, $\nabla^2 A_z + k_0^2 A_z = -\mu_0 J$, and the continuity equation to get the following circuit equation:

$$\left(-\beta_x^2 - \beta_y^2 - \beta^2 + k_0^2\right) A_z = -\frac{\mu_0 \omega}{\beta}\int_{-\infty}^{\infty} f_{\rm RF}(z, v, t) dv. \tag{15}$$

Using

$$E_z = \frac{k_0^2 - \beta^2}{j\omega\mu_0\varepsilon} A_z \tag{16}$$

which follows from the Lorentz gauge $\vec{\nabla}\cdot\vec{A} = -(1/(\varepsilon_r c^2))((\partial\Phi)/(\partial t))$, we obtain:

$$E_z = \frac{\beta_x^2 + \beta_y^2}{k_0^2 - \beta_x^2 - \beta_y^2 - \beta^2}\frac{j}{\varepsilon\beta}\int_{-\infty}^{\infty} f_{\rm RF}(z, v, t)\, dv \tag{17}$$

as the circuit equation. Combining this with the electronic equation and integrating by parts gives the quasi-linear dispersion relation

$$\left(\beta_1^2 - \beta^2\right) = -\left(\beta_x^2 + \beta_y^2\right)\frac{e}{m\varepsilon}\int_{-\infty}^{\infty}\frac{f_{\rm dc}(v)}{(\omega - \beta v)^2}\, dv. \tag{18}$$

After integration using a waterbag distribution (i.e., $f = \rho_0/2v_{\rm th}$ for the interval $v_{\rm beam} - v_{\rm th} \le v \le v_{\rm beam} + v_{\rm th}$), we have this dispersion relation

$$\left(\beta_1^2 - \beta^2\right)\left[\left(\frac{\omega}{v_{\rm beam}} - \beta\right)^2 - \frac{v_{\rm th}^2\beta^2}{v_{\rm beam}^2}\right] = 2\beta_1^4 C^3. \tag{19}$$

Here, we have used $I_{\rm beam} = \rho_0 ab v_{\rm beam}$, the fields for the $\rm TM_{11}$ mode in a dielectric filled waveguide, and have defined the Pierce parameter as before by $C^3 = I_{\rm beam}K_{\rm int}/4V_{\rm beam}$, where $K_{\rm int} = ((\pi^2)/(\varepsilon_r\varepsilon_0\omega))(1/((\omega/v_{\rm beam})^3))(((1/(a^2)) + (1/(b^2)))/(ab))$ (there is a factor of four decrease relative to (10), because the beam is no longer concentrated at the field maximum and we are ignoring the cosh term altogether). Importantly, a normal-mode derivation [17] yields the same form of the dispersion relation and the nature of the decrease in gain due to a velocity distribution as shown in (19) is general. We can identify the term depending on $v_{\rm th}$ in (19) as equivalent to Pierce's space charge term $4QC$, where $4QC = v_{\rm th}^2/\beta v_{\rm beam}^2 C^3$. The solution for this form of a dispersion relation is well known, with the gain being [23], [24]

$$j\beta_{\rm imag} = j\beta_1 C\frac{\sqrt{3}}{2}\left[1 - \left(\frac{v_{\rm th}}{3Cv_{\rm beam}}\right)^2\right]. \tag{20}$$

The rms velocity deviation from $v_{\rm beam}$ for a waterbag distribution is $v_{\rm rms} = v_{\rm th}/\sqrt{3}$; so, we can rewrite (20) in terms of the rms velocity deviation as

$$j\beta_{\rm imag} = j\beta_1 C\frac{\sqrt{3}}{2}\left[1 - \left(\frac{v_{\rm rms}}{\sqrt{3}Cv_{\rm beam}}\right)^2\right] \tag{21}$$

where, as stated earlier, we assume that the exact distribution does not largely effect the decrease in gain. The gain is affected as the velocity spread approaches $\sqrt{3}Cv_{\rm beam}$.

Next, we calculate the rms energy spread induced from the emittance. For a monoenergetic beam, the axial velocity is related to the vertical velocity by $v_z^2 = v_{\rm beam}^2 - v_y^2$, where $v_{\rm beam}^2 = 2\ eV/m$, we are ignoring the beam's potential depression, and V is the electron gun voltage. The beam is less (if at all) confined horizontally so the horizontal divergence can be ignored.

To calculate $v_{\rm rms}$, we first find the average beam axial velocity in terms of the vertical rms velocity which we assume has a normal distribution about $v_y = 0$ with variance σ_v. The deviation in axial velocity from $v_{\rm beam}$ is $\Delta v_z = -v_y^2/2v_{\rm beam}$. Integrating over the vertical velocity distribution, we find the

average deviation to be $\Delta v_{z,\mathrm{ave}} = -\sigma_v^2/2v_{\mathrm{beam}}$. The axial rms velocity spread is then

$$v_{\mathrm{rms}} = \sqrt{\langle \Delta v_z^2 \rangle - (\Delta v_{z,\mathrm{ave}})^2} = \sigma_v^2/\sqrt{2}v_{\mathrm{beam}}. \tag{22}$$

From the definition of emittance (1), we obtain $\sigma_v = \varepsilon_{y,\mathrm{norm}}c/Y$ or

$$\frac{v_{\mathrm{rms}}}{v_{\mathrm{beam}}} = \frac{1}{2\sqrt{2}}\frac{\varepsilon_{y,\mathrm{norm}}^2}{Y^2}\left(\frac{mc^2}{eV}\right). \tag{23}$$

Thus, the gain is degraded if the emittance approaches

$$\varepsilon_{y,\mathrm{norm}} \sim \sqrt{2\sqrt{6}}\sqrt{\frac{eV}{mc^2}}YC^{1/2}. \tag{24}$$

For nominal values of $V = 20$ kV, $C = 0.009$, and $Y = 0.1$ mm, the emittance limit is ~ 4 μm.

VI. Emittance Growth During Transport

In Sections IV and V, we have shown that the beam emittance needs to be on the order of a couple of micrometers or less, for nominal *W*-band TWT parameters. This puts a limit on both the beam's initial emittance and the amount of allowable emittance growth during transport. In 1936, Scherzer [25] showed that the higher order radial focusing terms are always present in cylindrical magnetic lenses, leading to an unavoidable aberration in electron microscopes that limit resolution to 50 to 100 wavelengths. Appling his theory to beam transport, these aberrations can cause emittance growth. In this section, we will calculate the equivalent emittance growth from a wiggler field.

Using results from [13], the wiggler field for natural focusing is given by

$$\begin{aligned} B_z &= B_w \sinh(k_w y)\cos(k_w z) \\ B_y &= B_w \cosh(k_w y)\sin(k_w z) \end{aligned} \tag{25}$$

where $k_w = 2\pi/\lambda_w$. The horizontal velocity with no initial magnetic field on the cathode is given by the planar Busch's theorem [13]

$$v_x = \frac{eB_w}{mk_w}\cosh(k_w y)\cos(k_w z) \tag{26}$$

which leads to the following equation of motion:

$$y'' = y\left(\frac{eB_w}{mv_{\mathrm{beam}}}\right)^2\left(1 + \frac{(k_w y)^2}{2}\right)\cos^2(k_w z). \tag{27}$$

This nonlinearity is equivalent to that for cylindrical PPM focusing where the nonlinearity arises from the expansion of the off-axis field, given by $B_z(r,z) = B_0(z) - r^2 B_0''(z)/4$.

We make a worst case bound by calculating the nonlinear response to this force assuming that the electrons are fixed in vertical position. In reality, there would be vertical mixing in emittance-dominated transport. With this approximation, we consider the emittance growth from this nonlinear response

$$y'' = \left(\frac{eB_w k_w}{2mv_{\mathrm{beam}}}\right)^2 y^3. \tag{28}$$

For simplicity, we assume that the beam density is uniform within an elliptical cross section and we rewrite the wiggle magnetic field in terms of emittance from (2), leading to these rms quantities after a short drift of Δz

$$\langle y'^2 \rangle = (\Delta z)^2\left(\frac{c\varepsilon_{y,\mathrm{norm}}k_w}{2v_{\mathrm{beam}}Y^2}\right)^4 2Y^6 \tag{29}$$

and

$$\langle yy' \rangle = -\Delta z\left(\frac{c\varepsilon_{y,\mathrm{norm}}k_w}{2v_{\mathrm{beam}}Y^2}\right)^2 \frac{4}{3}Y^4. \tag{30}$$

The maximum emittance growth is then

$$(\Delta\varepsilon_{y,\mathrm{norm,max}})^2 = \frac{v_{\mathrm{beam}}^2}{c^2}(\Delta z)^2\left(\frac{c\varepsilon_{y,\mathrm{norm}}k_w}{2v_{\mathrm{beam}}Y^2}\right)^4 \frac{2}{9}Y^8 \tag{31}$$

or

$$\left.\frac{d\varepsilon_{y,\mathrm{norm}}}{dz}\right|_{\mathrm{max}} = \frac{\sqrt{2}\pi^2}{3}\frac{c}{v_{\mathrm{beam}}}\frac{\varepsilon_{y,\mathrm{norm}}^2}{\lambda_w^2}. \tag{32}$$

Note that the emittance growth is independent of beam size, and only depends on its velocity and emittance, and the wiggle period. For our nominal beam parameters (20 keV beam with an emittance of a few micrometers and a wiggle period of about (1/2) cm), we find an emittance growth rate of about 1 μm/cm which could be problematic for a TWT with 50 dB of gain over 10 cm. Even though this is an upper limit, it indicates that care must be taken with transport in a wiggler as short at 10 cm. Note that small emittances will strongly suppress this emittance growth mechanism, again indicating the need for submicrometer beam emittances.

VII. Conclusion

We have considered the two key emittance effects relevant to high-frequency TWTs for the case of low beam voltages requiring a sheet electron beam for high power. For our example sheet-beam *W*-band TWT parameters, the emittance limit for stable transport in a periodic focusing structure is about 1 μm. Also, the nominal tube gain of about 5 dB/cm is liable to degrade if the emittance exceeds much over 1 μm. In addition, we found that beam emittances much larger than 1 μm will stimulate even greater emittance growth in transit.

Although this analysis was done for our nominal beam and TWT parameters, these results are general. Note that the emittance limit is lower at higher frequency, because the beam size scales proportional with wavelength (at least in one dimension). From (24), we directly see that the beam emittance needs to decrease linearly with wavelength to avoid gain degradation (assuming C stays constant). The emittance dependence for stable transport is more complicated, but ends up with roughly the same scaling. From (10), $B_w\lambda_w$ should be kept constant. Assuming all sizes (including the wiggler dimensions) scale with wavelength, the wiggler peak field can scale inversely with wavelength. From (1), the emittance also needs to scale with wavelength.

Roughly speaking, since the threshold emittance at *W*-band is about 1 μm, it is about 0.4 μm at 220 GHz and 0.1 μm at 1 THz.

Also, note from (32) that the scaling of the possible emittance growth from periodic focusing nonlinearities makes this effect worse at higher frequencies. To mitigate this, a quadrupole focusing lattice could be used (for either cylindrical or

sheet beams) [26], which would suppress this type of emittance growth.

A major consequence of this analysis is the observation that conventional cylindrical thermionic guns and guns using field emitters will likely not be suitable for high-power (i.e., high current) TWTs at W-band and higher frequencies. References [7], [8] show that the cylindrical low-perveance nongridded guns have emittances of 2 μm to a few μm and field emitter guns have emittances of about 10 μm. The required reduction in beam emittance can be achieved by increasing the current density on the cathode for cylindrical guns [see the scaling in (3)], using an elliptical cathode geometry [27], [28], or by using an emittance partitioning scheme like a flat beam transform (FBT) [29], [30]. An FBT design approach for a thermionic gun suitable for a W-band TWT was given in [31].

REFERENCES

[1] J. Cai, J. Feng, Y. Hu, X. Wu, Y. Du, and J. Liu, "10 GHz bandwidth 100 watt W-band folded waveguide pulsed TWTs," *IEEE Microw. Wireless Compon. Lett.*, vol. 24, no. 9, pp. 620–621, Sep. 2014.

[2] C. D. Joye *et al.*, "Demonstration of a high-power, wideband 220-GHz traveling-wave amplifier fabricated by UV-LIGA," *IEEE Trans. Electron Devices*, vol. 61, no. 6, pp. 1672–1678, Jun. 2014.

[3] K. T. Nguyen, "Design methodology and experimental verification of serpentine/folded waveguide TWTs," *IEEE Trans. Electron Devices*, vol. 61, no. 6, pp. 1679–1686, Jun. 2014.

[4] J. Pasour *et al.*, "Demonstration of a multikilowatt, solenoidally focused sheet beam amplifier at 94 GHz," *IEEE Trans. Electron Devices*, vol. 61, no. 6, pp. 1630–1636, Jun. 2014.

[5] E. J. Kowalski, M. A. Shapiro, and R. J. Temkin, "An overmoded W-band coupled-cavity TWT," *IEEE Trans. Electron Devices*, vol. 62, no. 5, pp. 1609–1616, May 2015.

[6] M. Field *et al.*, "Development of a 220 GHz 50 W sheet beam travelling wave amplifier," in *Proc. IEEE Int. Vac. Electron. Conf.*, Apr. 2014, pp. 225–226.

[7] R. True, "Emittance and the design of beam formation, transport, and collection systems in periodically focused TWTs," *IEEE Trans. Electron Devices*, vol. 34, no. 2, pp. 473–485, Feb. 1987.

[8] D. R. Whaley, "Practical design of emittance dominated linear beams for RF amplifiers," *IEEE Trans. Electron Devices*, vol. 61, no. 6, pp. 1726–1734, Jun. 2014.

[9] B. E. Carlsten and K. E. Nichols, "Beam transport and beam-current loss in emittance-dominated W-band TWTs," to be published.

[10] P. Schmuser, M. Dohlus, and J. Rossbach, *Ultraviolet and Soft X-Ray Free-Electron Lasers*. New York, NY, USA: Springer-Verlag, 2008.

[11] E. I. Simakov *et al.*, "Ceramic structures and other test components for the 96 GHz mm-wave traveling wave tube," in *Proc. Proc. IEEE Int. Vac. Electron. Conf.*, Apr. 2016.

[12] E. I. Simakov *et al.*, "Design and fabrication of components for the 96 GHz traveling-wave tube experiment," to be published.

[13] B. E. Carlsten *et al.*, "Stability of an emittance-dominated sheet-electron beam in a planar wiggler and periodic permanent magnet structures with natural focusing," *Phys. Rev. ST Accel. Beams*, vol. 8, p. 062001, Jun. 2005.

[14] D. H. Dowell *et al.*, "Cathode R&D for future light sources," *Nucl. Instrum. Methods Phys. Res. A, Accel. Spectrom. Detect. Assoc. Equip.*, vol. 622, no. 3, pp. 685–697 Oct. 2010.

[15] B. Vancil, I. Brodie, J. Lorr, and V. Schmidt, "Scandate dispenser cathodes with sharp transition and their application in microwave tubes," *IEEE Trans. Electron Devices*, vol. 61, no. 6, pp. 1754–1759, Jun. 2014.

[16] *Computer Simulation Technology CST Microwave Studio*, accessed on Jul. 22, 2016. [Online]. Available: https://www.cst.com/Products/CSTMWS

[17] M. Chodorow and C. Susskind, *Fundamentals of Microwave Electronics*. New York, NY, USA: McGraw-Hill, 1964.

[18] K. T. Nguyen, J. A. Pasour, T. M. Antonsen, P. B. Larsen, J. J. Petillo, and B. Levush, "Intense sheet electron beam transport in a uniform solenoidal magnetic field," *IEEE Trans. Electron Devices*, vol. 56, no. 5, pp. 744–752, May 2009.

[19] K. Halbach, "Design of permanent multipole magnets with oriented rare earth cobalt material," *Nucl. Instrum. Methods*, vol. 169, no. 1, pp. 1–10, Feb. 1980.

[20] D. Watkins and D. Rynn, "Effects of velocity distribution on traveling wave tube gain," *J. Appl. Phys.*, vol. 25, no. 11, p. 1375, Feb. 1954.

[21] F. J. Sacherer, "RMS envelope equations with space charge," *IEEE Trans. Nucl. Sci.*, vol. 18, no. 3, pp. 1105–1107, Jun. 1971.

[22] M. Reiser, *Theory and Design of Charged Particle Beams*. New York, NY, USA: Wiley, 2008.

[23] J. R. Pierce, "Traveling-wave tubes," *Bell Labs Tech. J.*, vol. 29, no. 3, pp. 390–460 Jul. 1950.

[24] L. Schachter, *Beam-Wave Interaction in Periodic and Quasi-Periodic Structures*, 2nd ed. New York, NY, USA: Springer-Verlag, 2011.

[25] O. Scherzer, 'Uber einige Fehler von Elektronenlinsen," *Z. Phys.*, vol. 101, no. 9, pp. 593–603, Sep. 1936.

[26] K. Nichols, B. Carlsten, and E. Schamiloglu, "Analysis of quadrupole focusing lattices for electron beam transport in traveling-wave tubes," *IEEE Trans. Electron Devices*, vol. 61, no. 6, pp. 1865–1870, Jun. 2014.

[27] D. Sprehn, A. Haase, A. Jensen, E. Jongewaard, and D. Martin, "Test and development of a 10 MW 1.3 GHz sheet beam klystron for the ILC," in *Proc. Int. Particle Accel. Conf.*, Kyoto, Japan, 2010, pp. 4023–4025.

[28] R. Bhatt and C. Chen, "Theory and Simulation of nonrelativistic elliptic-beam formation with one-dimensional Child Langmuir flow characteristics," *Phys. Rev. ST Accel. Beams*, vol. 8, p. 014201, Jan. 2005.

[29] R. Brinkmann, Y. Derbenev, and K. Flottmann, "A low emittance, flat-beam electron source for linear colliders," *Phys. Rev. ST Accel. Beams*, vol. 4, p. 053501, May 2001.

[30] B. E. Carlsten *et al.*, "Arbitrary emittance partitioning between any two dimensions for electron beams," *Phys. Rev. ST Accel. Beams*, vol. 14, p. 050706, May 2011.

[31] B. E. Carlsten and K. A. Bishofberger, "Simple algorithm for designing skew quadrupole emittance converter configurations," *New J. Phys.*, vol. 8, no. 11, p. 286, 2006.

Bruce E. Carlsten (M'87–S'13–F'16) received the Ph.D. degree in electrical engineering from Stanford University in 1985, with a major in microwave electronics.

Since 1985, he has been with the Los Alamos National Laboratory, Los Alamos, NM, USA, conducting research on high-brightness electron beams, advanced accelerator technology, free-electron lasers, and novel RF sources. His current research interests include sheet beam W-band TWTs.

Dr. Carlsten is a fellow of the American Physical Society.

Kimberley E. Nichols was born in Kingston, Canada. She received the B.A. degree from St. John's College, Annapolis, MD, USA, in 2008, and the Ph.D. degree in engineering from the University of New Mexico in 2014, where she was involved with the Applied Electromagnetics Group under Dr. E. Schamiloglu.

She was with the Los Alamos National Laboratory, Los Alamos, NM, USA, as a Post-Doctoral Research Associate in 2014.

Dmitry Yu. Shchegolkov received the B.Sc. and M.Sc. degrees in physics and plasma physics from the N. I. Lobachevsky State University of Nizhny Novgorod, Nizhny Novgorod, Russia, in 2002 and 2004, respectively, and the Ph.D. degree in radio physics from the Institute of Applied Physics, Russian Academy of Sciences, Nizhny Novgorod, in 2007.

He is currently a Staff Scientist with the Los Alamos National Laboratory, Los Alamos, NM, USA.

Evgenya I. Simakov received the Ph.D. degree in physics from the Massachusetts Institute of Technology, Cambridge, MA, USA, in 2005.

She joined the Los Alamos National Laboratory, Los Alamos, NM, USA, in 2005, as a Staff Scientist. Her current research interests include advanced electromagnetic structures for accelerators, microwaves, and millimeter waves.

Dr. Simakov is a 2011 recipient of the Presidential Early Career Award for Scientists and Engineers.